Prolyl endopeptidase gene disruption attenuates high fat diet-induced nonalcoholic fatty liver disease in mice by improving hepatic steatosis and inflammation

Dai-Xi Jiang[#], Jian-Bin Zhang[#], Meng-Ting Li, Shuang-Zhe Lin, Yu-Qin Wang, Yuan-Wen Chen, Jian-Gao Fan

Department of Gastroenterology, Xinhua Hospital Affiliated to Shanghai Jiao Tong University School of Medicine, Shanghai 200092, China

Contributions: (I) Conception and design: YW Chen, YQ Wang, JG Fan; (II) Administrative support: None; (III) Provision of study materials or patients: None; (IV) Collection and assembly of data: DX Jiang, JB Zhang; (V) Data analysis and interpretation: DX Jiang, SZ Lin; (VI) Manuscript writing: All authors; (VII) Final approval of manuscript: All authors.

[#]These authors contributed equally to this work.

Correspondence to: Yuan-Wen Chen; Yu-Qin Wang. Department of Gastroenterology, Xinhua Hospital Affiliated to Shanghai Jiao Tong University School of Medicine, 1665 Kongjiang Road, Shanghai 200092, China. Email: chenyuanwen@xinhuamed.com.cn; wangyuqin@xinhuamed.com.cn.

Background: Prolyl endopeptidase (PREP) is a serine endopeptidase that regulates inflammatory responses. PREP inhibitors can reduce hepatocyte lipid accumulation and may participate in the progression of nonalcoholic fatty liver disease (NAFLD). We investigated whether disruption of PREP regulates hepatic steatosis and inflammation in mice with NAFLD.

Methods: Wild-type and PREP gene disrupted mice were randomly divided into low-fat diet wild-type (LFD-WT), high-fat diet wild-type (HFD-WT), low-fat diet PREP disruption (LFD-PREP^{gt}), and high-fat diet PREP disruption (HFD-PREP^{gt}) groups. Animals were euthanized at the endpoint of 32 weeks. The NAFLD activity score and number of inflammatory cells were determined by hematoxylin-eosin staining and immunohistochemical staining of liver tissue. The expression levels of inflammation- and lipid metabolism-associated genes in the liver and serum were detected by quantitative reverse transcription PCR, mass spectrometry, or enzyme-linked immunosorbent assay.

Results: The body weight and epididymal fat tissue index of the HFD-PREP^{gt} mice were significantly decreased compared with that of the HFD-WT mice. Moreover, the NAFLD activity score and liver function were attenuated in the HFD-PREP^{gt} mice. Fat accumulation and the level of expression of mRNAs associated with lipid metabolism and proinflammatory responses were improved in the HFD-PREP^{gt} mice. The number of CD68-positive cells in liver tissue and the serum levels of inflammation-associated factors were significantly decreased in the HFD-PREP^{gt} mice compared with those in the HFD-WT mice. Further mechanistic investigations indicated that the protective effect of PREP disruption on liver inflammation was associated with the suppressed production of matrix metalloproteinases (MMPs) and proline-glycine-proline (PGP) and the inhibition of neutrophil infiltration.

Conclusions: Loss of PREP lowers the severity of hepatic steatosis and inflammatory responses in a high-fat diet-induced nonalcoholic steatohepatitis model. PREP inhibition may protect against NAFLD.

Keywords: Liver; mice; nonalcoholic fatty liver disease (NAFLD); proline-glycine-proline (PGP); PREP gene knockout; prolyl endopeptidase

Submitted Oct 23, 2019. Accepted for publication Dec 27, 2019.

doi: 10.21037/atm.2020.01.14

View this article at: http://dx.doi.org/10.21037/atm.2020.01.14

Introduction

Nonalcoholic fatty liver disease (NAFLD) is the most common liver disease, with an estimated worldwide prevalence of approximately 25%; NAFLD is a health problem globally (1). The disease spectrum ranges from simple steatosis to nonalcoholic steatohepatitis (NASH) and fibrosis, ultimately leading to cirrhosis and carcinoma, which are becoming the leading reasons for liver transplantation (2,3). NAFLD is a multisystemic disease that is closely associated with insulin resistance, type 2 diabetes mellitus, obesity, hyperinsulinemia, and cardiovascular diseases (4-6). To date, no effective medical interventions exist that completely reverse the disease other than lifestyle changes and dietary alterations (7).

NASH is considered the progressive form of NAFLD and is characterized by liver steatosis, inflammation, hepatocellular injury, and hepatic fibrosis (8). The mechanism of NAFLD progression is poorly understood; the pathobiology of NAFLD was initially suggested to include two phases, i.e., hepatocyte damage (lipotoxicity) and tissue repair (inflammation/fibrosis). Excessive lipid accumulation in hepatocytes is the hallmark of NAFLD. Hepatocyte lipotoxicity evokes a primal sterile inflammatory response that aims to eliminate damaged cells and promote tissue repair (9). However, inflammatory factors and oxidative stress lead to additional damage to the liver and even apoptosis of hepatocytes (10). Apparently, it is important to inhibit hepatocyte steatosis and hepatic inflammation to prevent NAFLD, and especially NASH.

Prolyl endopeptidase (PREP), also called prolyl oligopeptidase (POP), is a cytosolic enzyme that can specifically hydrolyze prolyl-containing peptides smaller than 3 kDa at the C-termini of proline residues (11). A collagen-derived fragment, proline–glycine-proline (PGP), which is formed from collagen by the combined action of matrix metalloproteinases (MMPs) and PREP, was shown to have chemotactic effects on neutrophils (12,13). Emerging evidence suggests that PREP modulates several peptides, which in turn regulate inflammatory responses as summarized by Penttinen *et al.* (14). PREP has been found to be closely related to diabetes, inflammatory neurodegenerative diseases, and autoimmune diseases (15-18). Early studies have indicated that a PREP assay may be useful in the diagnosis of the severity of local joint inflammation (18). Recent studies have demonstrated that PREP levels can be used as indicators of the severity of cirrhosis and to assess the level of neuroinflammation in humans (17). In terms of metabolism, Kim *et al.* proposed that central PREP plays an important role in the regulation of glucose sensing and insulin and glucagon secretion (15). Moreover, our previous *in vitro* studies demonstrated that the expression of PREP increases with hepatocyte steatosis and that PREP inhibitors can significantly reduce intracellular lipid accumulation (19). However, the subsequent interactions between NAFLD and PREP and their potential mechanism in NAFLD and NASH require clarification.

Considering the function of PREP, we hypothesized that PREP disruption would ameliorate disorders of lipid metabolism and hepatic inflammation to prevent NAFLD progression. Our results showed that PREP disruption protects mice against high-fat diet (HFD)-induced lipid accumulation and inflammatory cell accumulation in the liver. Therefore, in this study, we demonstrate that PREP inhibition may play a beneficial role in relieving steatohepatitis and that PREP inhibition may protect against NAFLD.

Methods

Animal experiments

Wild-type (WT) C57BL/6J and PREP-disrupted ($PREP^{gt}$) mice were obtained from the Shanghai Model Organisms Center, Inc. This gene knockout mouse project uses CRISPR/Cas9 technology to repair mutations introduced by non-homologous recombination (20,21), resulting in frame-shifting of the PREP open reading frame and loss of function. The $PREP^{gt}$ mice used in this study carry a partial deletion of exon 3 of the PREP gene. Details are provided in the Methods section of the Supplementary materials (Supplementary File). All animals were raised in a controlled environment at 25±2 ℃ with a 12-h light-dark cycle. After acclimating to the environment for 1 week, the mice were randomly distributed into four groups. LFD-WT and LFD-$PREP^{gt}$ mice were fed a standard chow diet; HFD-WT and HFD-$PREP^{gt}$ mice were fed a high-fat diet (88% standard diet, 10% lard, and 2% cholesterol). The mice were fed these diets for 32 weeks and were allowed free access to food and water. At the end of the experiments, the mice were fasted for 12 h and weighed. Blood samples were collected before the animals were euthanized. All animals were euthanized by pentobarbital sodium injection for tissue collection. All animal experiment protocols were approved by the Institutional Animal Care and Use Committee of

Xinhua hospital affiliated to Shanghai Jiao Tong University School of Medicine (approval No. XHEC-F-2019-061).

Functional biochemical assays

Serum and liver biochemical markers, including total cholesterol (TC), triglycerides (TGs), high density lipoprotein cholesterol (HDL-C), low density lipoprotein cholesterol (LDL-C), alanine aminotransferase (ALT), aspartate aminotransferase (AST), alkaline phosphatase (ALP), and glucose were detected using an automated analyzer (Roche Cobasc702, Switzerland) according to the manufacturer's instructions. Fasting insulin levels in serum were measured by enzyme-linked immunosorbent assay (ELISA, Crystalchem, USA), and the homeostasis model assessment of insulin resistance (HOMA-IR) and insulin sensitivity index (ISI) were calculated for each mouse. The serum levels of interleukin-6 (IL-6), tumor necrosis factor-α (TNF-α), and chemokine (C-C motif) ligand 2 (CCL2) were determined by ELISA (Shanghai Westang Biotech, Inc., China). The levels of chemokine (C-X-C motif) ligand 1 (CXCL1) and chemokine (C-X-C motif) ligand 2 (CXCL2) in liver tissues were measured by ELISA (Shanghai Westang Biotech, Inc., China). Liver reactive oxygen species (ROS) production was measured by colorimetry using a mouse total active oxygen detection kit (Shanghai Westang Biotech, Inc., China). All samples and standards were processed according to the manufacturer's instructions.

Histological tissue analysis

Liver tissue was fixed in 4% paraformaldehyde, frozen in O.C.T, or snap-frozen in liquid nitrogen and stored at −80 ℃. Paraformaldehyde-fixed paraffin-embedded sections of the liver were stained with hematoxylin-eosin for pathological analysis. Frozen sections in O.C.T were stained with Oil-Red-O to detect lipids. Images were captured by an optical microscope (Olympus BX51, China). The NAFLD activity score (NAS, 0-8 points) was assessed according to hepatic steatosis, lobular inflammation, and hepatocyte ballooning. A NAS <3 excludes NASH, NAS ≥5 can be used to diagnose NASH, and NAS between 3 and 5 indicates possible NASH. For immunohistochemistry, paraffin-embedded liver sections were stained with anti-CD68 antibody (ab125212, Abcam, USA), MPO antibody (gb11224, Servicebio, China), and Lipocalin-2 (LCN2) antibody (ab216462, Abcam, USA). Immunopositive cells were counted, and the number of positive cells in the liver sections was normalized to the tissue area.

Triglyceride and cholesterol evaluation in the liver

Liver levels of TGs and TC were detected by a triglyceride assay kit and a cholesterol assay kit, respectively (Applygen Technologies, Inc., Beijing, China), according to the manufacturer's instructions. The final concentrations of TGs and TC were normalized to protein content.

Quantitative reverse transcription polymerase chain reaction

Total RNA was extracted from the liver using TRIzol reagent (D9108B, Takara, Dalian, China) and converted into cDNA with reverse transcriptase (RR036A, Takara, Dalian, China). To quantify mRNA expression, quantitative polymerase chain reaction was performed using an Applied Biosystems ViiA7 real-time PCR system using SYBR Premix Ex Taq (Tli RNase H Plus) (RR420A, Takara, Dalian, China). The primers for the target genes were synthesized by Sangon Biotech (Shanghai, China) and are listed in *Table S1*. Glyceraldehyde 3-phosphate dehydrogenase (GAPDH) was used as an internal control. Relative mRNA expression levels were determined using the $2^{-\Delta\Delta Ct}$ method.

Western blotting

Liver tissue was lysed in ice-cold lysis buffer (Beyotime, China) containing protease inhibitors (Beyotime, Shanghai, China). Total protein was measured using a bicinchoninic acid protein assay (Beyotime, China). Then, the lysates were loaded onto 10% SDS-polyacrylamide gels. After electrophoresis, the protein was transferred onto a polyvinylidene difluoride (PVDF) membrane and sequentially detected by primary antibodies, secondary antibodies, and enhanced chemiluminescence. Rabbit anti-PREP (ab58988, Abcam, USA), anti-CD68 (ab125212, Abcam, USA), anti-MMP8 (ab81286, Abcam, USA), anti-MMP9 (ab38898, Abcam, USA), anti-LCN2 (ab216462, Abcam, USA), anti-PERK1/2 (4370T, Cell Signaling Technology, USA), and anti-ERK1/2 (4695T, Cell Signaling Technology, USA) antibodies were used. An anti-GAPDH antibody (AF0006, Beyotime, China) was used for detection

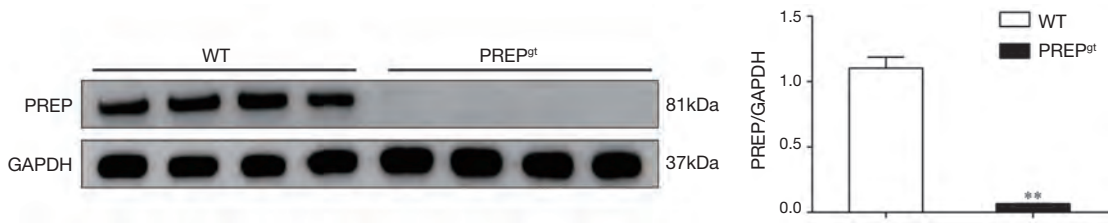

Figure 1 Representative anti-PREP western blot of the liver of WT and PREP^{gt} mice (upper panel) and blots of the GAPDH loading control (lower panel). Bar graphs display the quantification of the blots. **, P<0.01, WT *vs.* PREP^{gt}. WT, wild-type; PREP, prolyl endopeptidase.

of the internal control. The bands were quantified using Image Lab Version 2.0.1 (Bio-Rad, Hercules, CA).

Measurement of PGP and N-acetyl-PGP (N-Ac-PGP)

Each mouse sample was weighed (~50 mg) in a 2 mL centrifuge tube and 800 µL methanol/acetonitrile (1:1, v/v) was added. The samples were subjected to ultrasonication at 4 ℃ for 30 min and then were placed in a –20 ℃ freezer for 1 h. The mixture was centrifuged at 4 ℃ and the supernatant was transferred to the injection flask. The supernatant was analyzed using an API5500 QQQ – MS and Waters Acquity UPLC system. The UPLC column was an ACQUITY UPLC BEH HILIC (100 mm × 2.1 mm, d_p =1.7 µm) with a mobile phase of 0.2% formic acid and acetonitrile running at 0.7 mL/min. Positive electrospray mass transitions were monitored at 270>70 and 270>116 for PGP and at 312>140, 312>112, and 312>70 for N-Ac-PGP.

Statistical analysis

All data are expressed as the means ± SEM. Comparisons were performed using one-way analysis of variance (ANOVA) in GraphPad Prism 6. Tukey's post-hoc comparisons were used to compare multiple experimental groups. P<0.05 was considered to be statistically significant.

Results

PREP disruption ameliorates weight gain and metabolic disturbance in HFD-fed mice

The PREP^{gt} mice used in this study carry a partial deletion in exon 3 of the PREP gene that causes a complete loss of immunodetectable PREP protein in the liver. *Figure 1* shows representative PREP western blots.

We explored the role of PREP in NAFLD using PREP^{gt} and WT C57BL/6J mice after 32 weeks of HFD. Under low-fat diet conditions, the majority of the parameters related to NAFLD and metabolic homeostasis of the PREP^{gt} mice did not significantly differ from those of the WT mice. After HFD feeding for 32 weeks, the WT mice but not the PREP^{gt} mice had an enlarged and paler liver (*Figure 2A*). Specifically, the HFD-PREP^{gt} mice gained less body weight than the HFD-WT mice without a reduction in energy intake (*Figure 2B,C*). Additionally, the HFD-WT mice had significantly higher epididymal fat indices than the HFD-PREP^{gt} mice, but the liver indices were similar between the groups (*Figure 2C*). Consistently, the HFD-PREP^{gt} mice did not exhibit elevated serum fasting insulin levels or a higher HOMA-IR, while the HFD-WT mice did (*Figure 2D*). However, PREP disruption had no effect on the ISI and fasting blood glucose (*Figure 2D*). The serum levels of ALT, AST, and ALP in the HFD-WT mice were significantly higher than those in the LFD-WT and HFD-PREP^{gt} mice. However, there were no significant differences in the blood lipid parameters between the HFD-WT and HFD-PREP^{gt} mice, except for TGs (*Table 1*).

Fat accumulation and lipid metabolism improved in the livers of HFD-PREP^{gt} mice

Hematoxylin-eosin staining demonstrated substantially increased fat accumulation in the livers of the HFD-WT mice after 32 weeks compared with that in the LFD-WT or HFD-PREP^{gt} mice. NAS (7.75±0.16 *vs.* 0.17±0.17 or 4.88±0.51, respectively), steatosis (3.00±0 *vs.* 0 or 1.12±0.23, respectively), inflammation (2.63±0.18 *vs.* 0 or 1.88±0.35, respectively), and ballooning scores (2.00±0 *vs.* 0.83±0.17

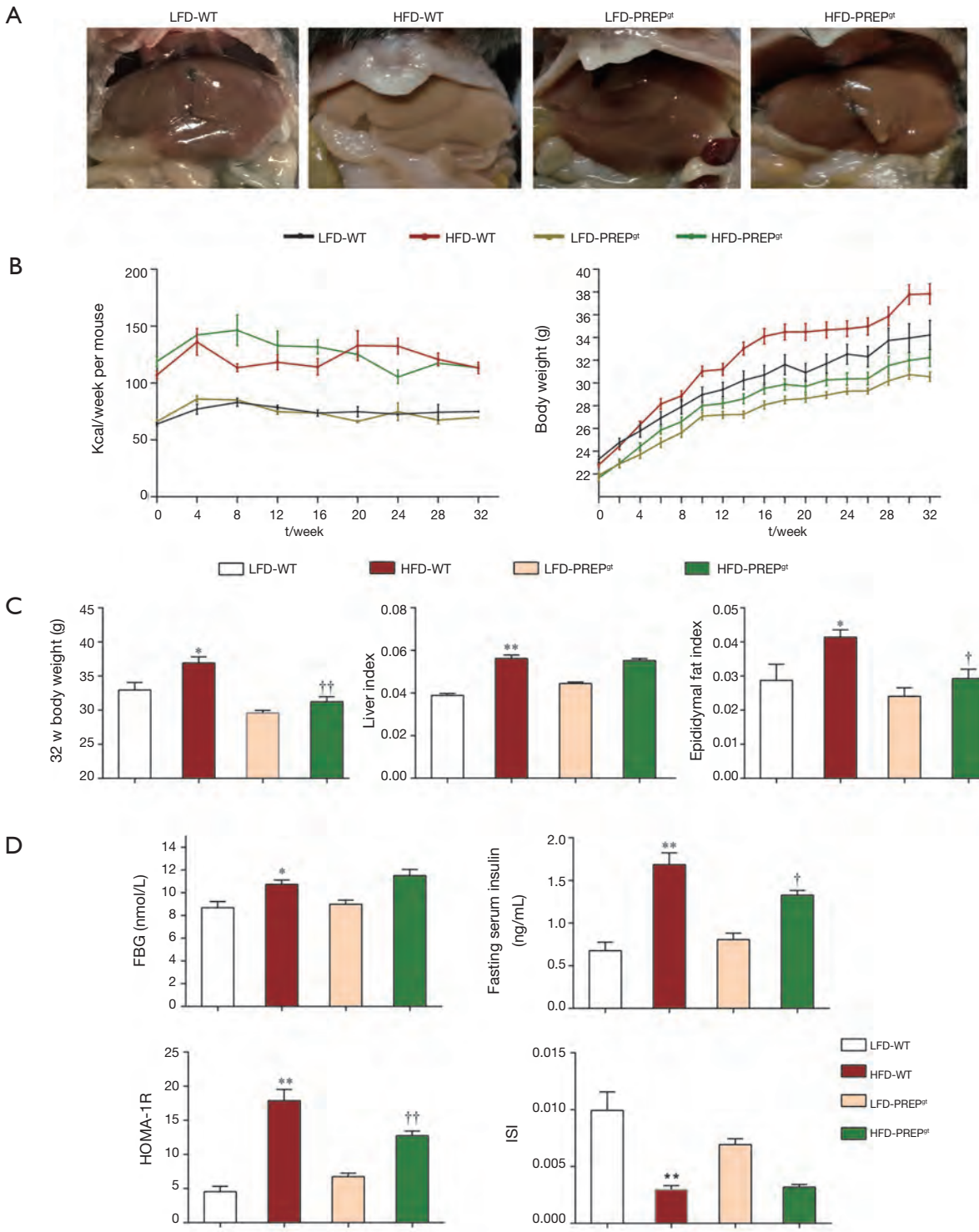

Figure 2 PREP disruption attenuates high-fat diet-induced obesity and metabolic disturbance. (A) Gross appearances of the livers of the LFD-WT, HFD-WT, LFD-PREP^{gt}, and HFD-PREP^{gt} groups; (B) body weight changes and energy intake per mouse per week; (C) liver index (liver weight/body weight) and epididymal fat index (epididymal fat weight/body weight); (D) fasting serum glucose, fasting serum insulin, HOMA-IR, and ISI of the four groups. All data are the means ± SEM (n=6–8). **P<0.01, LFD-WT *vs.* HFD-WT; ††P<0.01, HFD-WT *vs.* HFD-PREP^{gt}. HFD, high-fat diet; LFD, low-fat diet. WT, wild-type; PREP, prolyl endopeptidase.

Table 1 Summary of serum biomarkers in mice

	WT		PREP^{gt}	
	LFD (n=10)	HFD (n=14)	LFD (n=9)	HFD (n=12)
ALT (U/L)	28.26±2.41	122.00±52.94**	37.33±24.84	78.70±31.67†
AST (U/L)	92.94±9.74	137.29±27.15**	110.44±27.73	112.82±16.96†
ALP (U/L)	67±9.1	106.43±30.66**	60.00±7.68	84.17±20.98†
LDL-C (mmol/L)	0.18±0.07	0.58±0.08**	0.18±0.02	0.74±0.29
HDL-C (mmol/L)	2.92±0.39	3.71±0.43**	3.25±0.17	3.53±0.43
TC (mmol/L)	3.35±0.33	4.62±0.44**	3.70±0.20	4.70±0.48
TG (mmol/L)	1.01±0.15	0.90±0.10*	1.12±0.10	0.78±0.12†

*P<0.05 and **P<0.01, LFD-WT *vs*. HFD-WT; †P<0.05, HFD-WT *vs*. HFD-PREP^{gt}. WT, wild-type; PREP, prolyl endopeptidase; HFD, high-fat diet; LFD, low-fat diet; ALT, alanine aminotransferase; AST, aspartate aminotransferase; ALP, alkaline phosphatase; LDL-C, low density lipoprotein cholesterol; HDL-C, high density lipoprotein cholesterol; TC, total cholesterol; TG, triglyceride.

Table 2 Comparison of NAS in each group

Group	N	Steatosis	Ballooning	Lobular inflammation	NAS
LFD-WT	10	0.17±0.17	0.83±0.17	0.00	1.17±0.17
HFD-WT	14	3.00±0**	2.00±0**	2.63±0.18**	7.75±0.16**
LFD-PREP^{gt}	9	0.00± 0.0	1.00±0.00	0.50±0.34	1.50±0.34
HFD-PREP^{gt}	12	1.12±0.23††	1.88±0.13††	1.88±0.35††	4.88±0.51††

**P<0.01, LFD-WT *vs*. HFD-WT; ††P<0.01, HFD-WT *vs*. HFD-PREP^{gt}. WT, wild-type; PREP, prolyl endopeptidase; HFD, high-fat diet; LFD, low-fat diet.

or 1.88±0.13, respectively) were substantially increased in the HFD-WT mice compared with those in the LFD-WT or HFD-PREP^{gt} mice (*Table 2* and *Figure 3A*). As shown with Oil-Red-O staining, lipid droplet accumulation in the liver was markedly decreased in the HFD-PREP^{gt} mice than in the HFD-WT mice (*Figure 3A*). As confirmation, the hepatic levels of TGs (594.4±98.57 *vs*. 1181±69.10, respectively) and TC (710.1±24.74 *vs*. 938.4±38.76, respectively) were significantly lower in the HFD-PREP^{gt} mice than in the HFD-WT mice (*Figure 3B*).

Regarding the genes and enzymes involved in fat metabolism, the liver mRNA levels of lipid synthesis enzymes, such as acetyl-coenzyme A carboxylase (ACC), fatty acid synthase (FAS), and stearoyl-CoA desaturase 1 (SCD1), in the HFD-WT mice were significantly higher than the corresponding levels in the LFD-WT and HFD-PREP^{gt} mice (*Figure 3C*). We also observed a significant downregulation of ACOX1 (the initial enzyme of peroxisomal β-oxidation) in the livers of the HFD-PREP^{gt} mice compared with that in the HFD-WT mice (*Figure 3C*). ROS production was consistent with the ACOX1 results (*Figure 3D*). The level of CD36, but not FABP1, was substantially upregulated in the livers of the HFD-WT mice compared with that in the livers of the LFD-WT mice; however, the levels of CD36 and FABP1 were substantially improved in the HFD-PREP^{gt} mice (*Figure 3E*). The PPAR-γ level was significantly higher in the HFD-WT mice than in the LFD-WT mice, but it was downregulated in the HFD-PREP^{gt} mice (*Figure 3F*). However, the level of PPAR-α expression in the livers of the HFD-WT mice was higher than that in the LFD-WT and HFD-PREP^{gt} mice, but the values were not significantly different (*Figure 3F*). PREP gene disruption reduced the levels of these mRNAs in the HFD mice to those observed in the LFD-WT mice.

PREP disruption inhibits hepatic macrophage accumulation and decreases the severity of HFD-induced proinflammatory responses in the liver

The number of hepatic macrophages normalized to

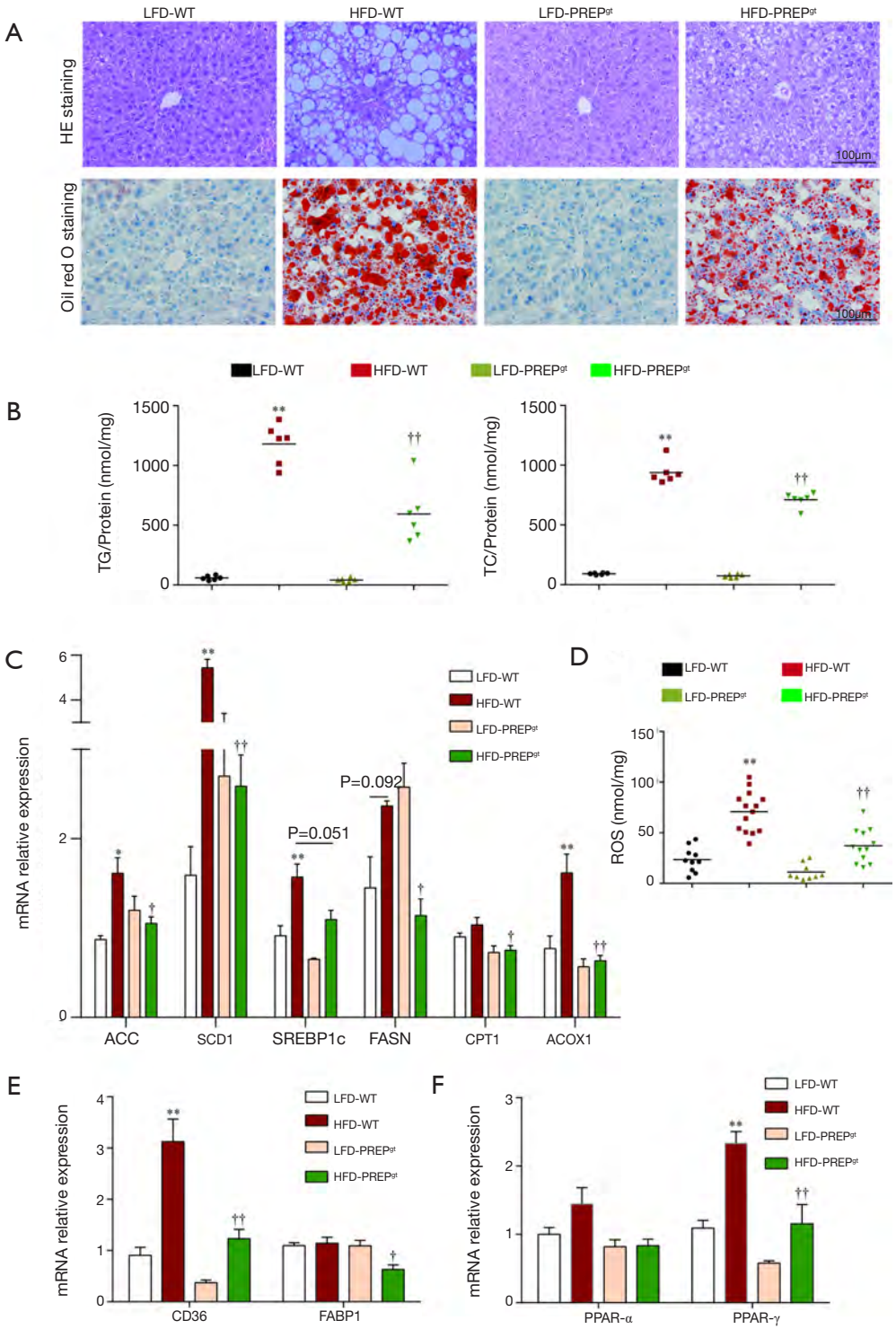

Figure 3 Improved fat accumulation and lipid metabolism in the livers of HFD-PREP^{gt} mice. (A) Liver sections were stained with hematoxylin-eosin and Oil-Red-O (200× magnification); (B) hepatic levels of triglycerides and cholesterol; (C) hepatic mRNA levels of lipid synthesis-associated genes were examined using quantitative reverse transcription polymerase chain reaction; (D) production of ROS in the liver; (E) fatty acid transport-associated CD36 and FABP1; (F) expression of the lipid metabolism-associated PPAR-α and PPAR-γ genes. Gene expression levels are expressed relative to the control group. All data are presented as the means ± SEM (n=6–8). *P<0.05 and **P<0.01, LFD-WT *vs.* HFD-WT; †P<0.05, HFD-WT *vs.* HFD-PREP^{gt}. WT, wild-type; PREP, prolyl endopeptidase; HFD, high-fat diet; LFD, low-fat diet.

the tissue area was significantly increased in the HFD-WT mice (34.50±2.613) compared with that in the LFD-WT mice (1.104±0.5164) according to CD68 immunohistochemistry (*Figure 4A*). However, a reduction in the number of hepatic macrophages was observed in the HFD-PREP^{gt} mice (18.49±2.135) and was associated with a significant reduction in CD68 protein expression in the liver (*Figure 4B*). Specifically, the HFD-PREP^{gt} mice had a pronounced downregulation of CCL2 and CCR2 gene expression compared with that of the HFD-WT mice (*Figure 4C*). Additionally, the mRNA expression levels of other proinflammatory cytokines were enhanced in the livers of the HFD-WT mice, namely TNF-α, IL-6, IL-1β, CCL5, and all of the cytokines that are ameliorated in the HFD-PREP^{gt} mice (*Figure 4C*). Moreover, the serum levels of IL-6, TNF-α, and CCL2 in the HFD-WT mice were higher than those in the LFD-WT mice, and these differences were statistically significant (*Figure 4D*). A substantial decrease in cytokine levels was detected in the HFD-PREP^{gt} mice (*Figure 4D*).

PREP disruption suppresses production of MMPs and PGP and inhibits neutrophil infiltration

The number of hepatic neutrophils normalized to the tissue area was significantly increased in the HFD-WT mice (54.50±5.571) compared with that in the LFD-WT mice (4.113±1.679) according to MPO immunohistochemistry (*Figure 5A*). In addition, a reduction in the number of hepatic neutrophils was observed in the HFD-PREP^{gt} mice (24.34±5.275) (*Figure 5A*). The results of LCN2 protein expression and immunohistochemistry in the liver sections were consistent with the MPO immunohistochemistry results (*Figure 5A*,*B*). The combined action of MMPs and PREP is responsible for the cleavage of collagen to generate PGP, which was shown to have chemotactic effects on neutrophils. Specifically, western blot results showed that the protein expression levels of MMP8 and MMP9 were significantly lower in the HFD-PREP^{gt} mice than in the HFD-WT mice (*Figure 5B*). In addition, the production of PGP with HFD stimulus was obviously suppressed after PREP disruption (*Figure 5C*). The production of N-Ac-PGP also decreased in the HFD-PREP^{gt} mice but the mean value was not significantly different from that in the HFD-WT mice (*Figure 5C*). Moreover, we found that the levels of CXCL1 and CXCL2 were significantly decreased in the livers of the HFD-PREP^{gt} mice compared with those in the HFD-WT mice (*Figure 5D*). We also assessed the mRNA expression of CXCR2, which was ameliorated in the HFD-PREP^{gt} mice; however, the values were not significantly different from those of the HFD-WT mice (*Figure S1*). Western blotting analysis showed that neutrophil-activation-associated phosphorylation of ERK1/2 was markedly inhibited in the livers of the HFD-PREP^{gt} mice compared with that in the HFD-WT mice (*Figure 5B*).

Discussion

NASH has become a major cause of cirrhosis and liver-related deaths worldwide, and the incidence of NAFLD-related liver disease in adults and children is continuously increasing because of ongoing obesity epidemics (9,22). Emerging evidence indicates that PREP regulates inflammatory responses and lipid accumulation (14,19). In the present study, we observed that disruption of PREP ameliorates weight gain, metabolism, and HFD-induced impairment of liver function. PREP knockout alleviates the changes in hepatic lipid metabolism and inflammatory cell accumulation observed in our experiments. Thus, our data illustrate that PREP knockout alleviates the progression of NASH.

Our results demonstrate that PREP disruption decreases HFD-induced weight gain without a reduction in energy intake. Hofling *et al.* suggested that a deficiency in PREP can cause a reduction in body weight and anxiety while enhancing hyperactivity (23), which may explain the phenomenon. The serum levels of ALP, AST, and ALP were significantly decreased in the HFD-PREP^{gt} mice compared with those in the HFD-WT mice, indicating that PREP disruption plays a protective role in liver function in the NASH model. Serum insulin levels and HOMA-IR were significantly decreased in the HFD-PREP^{gt} mice compared with those in the HFD-WT mice. However, fasting glucose levels were not significantly different between the HFD-WT and HFD-PREP^{gt} mice. These findings are in partial disagreement with a previous study that showed that PREP knockdown mice exhibited glucose intolerance, decreased fasting insulin levels, increased fasting glucagon levels, and reduced glucose-induced insulin secretion compared with the corresponding levels in wild-type controls fed a standard chow diet (15). However, another study showed that inhibition of the PREP subfamily member, fibroblast activation protein, provided robust metabolic benefits in obese mice that were not observed in lean animals (24). Therefore, the methodological differences between our study and these other studies should not be ignored. We

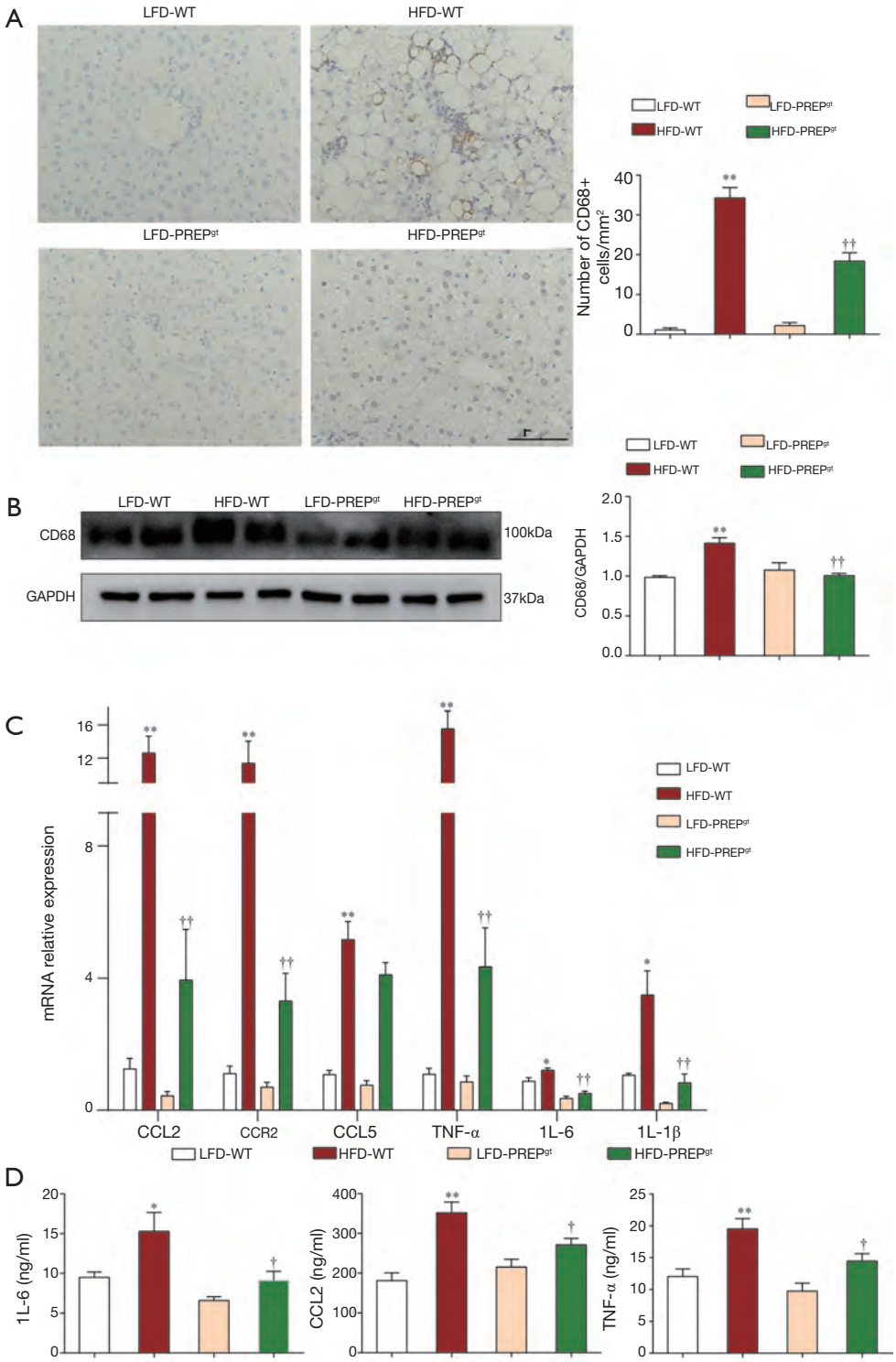

Figure 4 PREP disruption inhibits hepatic macrophage accumulation and improves the severity of hepatic inflammation. (A) Liver sections were stained with anti-CD68 (200× magnification); (B) protein levels of CD68 were detected using western blot analysis; (C) expression of proinflammatory cytokine mRNAs; (D) protein levels of proinflammatory cytokines measured by ELISA. All data are presented as the means ± SEM (n=6–8). *P<0.05 and **P<0.01, LFD-WT *vs.* HFD-WT; †P<0.05 and ††P<0.01, HFD-WT *vs.* HFD-PREP^{gt}. WT, wild-type; PREP, prolyl endopeptidase; HFD, high-fat diet; LFD, low-fat diet.

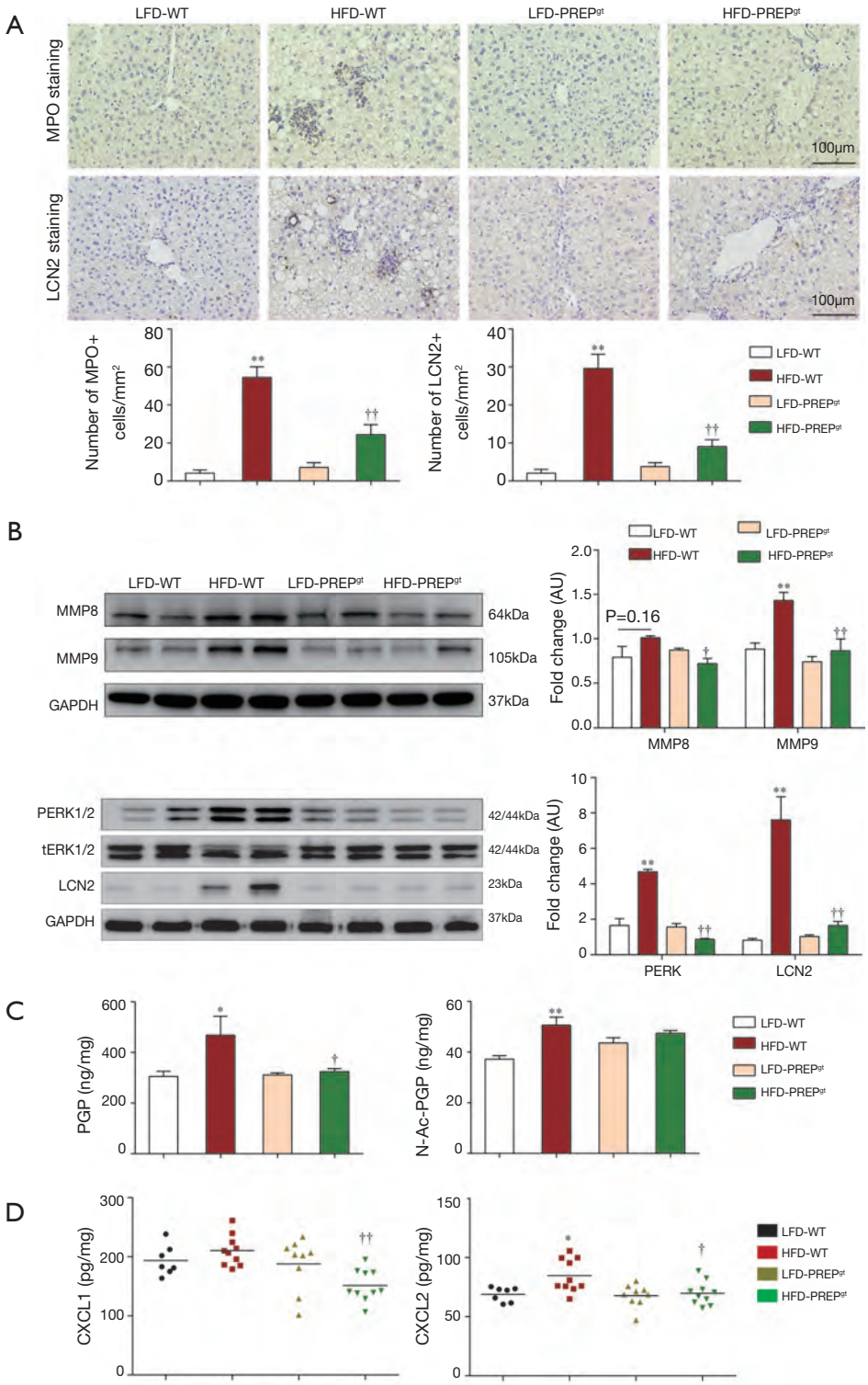

Figure 5 PREP disruption inhibits neutrophil infiltration and suppresses the production of MMPs and PGP. (A) Liver sections stained with anti-MPO and anti-LCN2 (200× magnification); (B) protein levels of MMP8/9, PERK1/2, and LCN2 detected using western blot analysis; (C) hepatic N-Ac-PGP and PGP levels in different groups; (D) hepatic protein levels of CXCL1/CXCL2 measured by ELISA. All data are presented as the means ± SEM (n=6–8). *P<0.05 and **P<0.01, LFD-WT *vs.* HFD-WT; †P<0.05 and ††P<0.01, HFD-WT *vs.* HFD-PREP^{gt}. WT, wild-type; PREP, prolyl endopeptidase; HFD, high-fat diet; LFD, low-fat diet.

hypothesize that PREP knockout has protective effects with regard to the regulation of glucose metabolism and pancreatic function upon HFD stimulus, and further studies are needed to investigate these possibilities.

Obesity is a known risk factor for NASH. This risk factor has been attributed to visceral adipose tissue expansion associated with inflammation (25). Increased fatty acid flow to hepatocytes from the adipose tissue and diet and increased *de novo* lipogenesis in liver cells are the main factors that promote hepatic TG synthesis and TC accumulation, resulting in lipotoxicity (9,26). Our study demonstrates that PREP disruption reduces visceral adipose tissue, downregulates free fatty acid transporters (CD36 and FABP1), and improves *de novo* lipogenesis (ACC, FASN, SREBP1c, and SCD1) in the animal model of steatohepatitis. These findings are consistent with our previous cytology study, which revealed that the expression levels of FASN and SREBP1c, the key genes in the synthesis of endogenous long chain fatty acids, were significantly decreased after PREP inhibition (19). Another study described that POP inhibition in the liver alters the turnover of mitochondrial proteins, which may influence ATP synthesis via various proteins, such as cytochrome C oxidase and ATP synthase; this inhibition can be an essential factor in the alleviation of hepatic steatosis by PREP knockout observed in the present study (27). In agreement with this suggestion, we observed a significant downregulation of ACOX1, the initial enzyme of peroxisomal β-oxidation, in HFD-PREP^{gt} liver tissue. This type of fatty acid catabolism causes an increase in hydrogen peroxide generation, which contributes to harmful ROS production in addition to impairment of the respiratory chain (28). Moreover, we observed that the expression of PPAR-γ, a key gene in the regulation of lipid metabolism, is decreased in the HFD-PREP^{gt} mice. This decrease may be mediated by the nuclear translocation of PREP, which can directly regulate the expression of genes related to adipogenic proteins (19). Based on these data, we conclude that PREP disruption can attenuate hepatic *de novo* lipogenesis, thus reducing hepatic lipid accumulation.

Hepatic inflammation is the key to the progression of NAFLD to NASH. A recent study investigated neuroinflammatory conditions and demonstrated that a PREP inhibitor, KYP-2047, significantly protected neurons against the toxicity of microglia (macrophage-like glial cells) and reduced the levels of the proinflammatory cytokine TNF-α (29). These data on neuroprotective effects are in agreement with the findings of Klegeris *et al.* (30). Another study demonstrated that PREP may play a role in microglial activation since PREP knockout mice lack a response to lipopolysaccharides at behavioral and immunohistochemical levels (23). Based on the findings that indicate that PREP promotes the activation of macrophage-like glial cells, we hypothesized that PREP disruption inhibits the accumulation of hepatic macrophages, thus decreasing the severity of HFD-induced hepatic inflammation. We tested this hypothesis by performing CD68 immunohistochemistry staining of liver sections and measured the levels of proinflammatory cytokines in liver tissue and serum. Circulating inflammatory monocytes are attracted to the injured liver through their chemokine receptor CCR2, while CCL2 is expressed at high levels in various liver cells, including activated Kupffer cells and damaged hepatocytes. Notably, the expression levels of CCL2 and its receptor were substantially downregulated in the HFD-PREP^{gt} mice. Furthermore, other proinflammatory factors in the liver (CCL5, TNF-α, IL-6, and IL-1β) and serum (CCL2, TNF-α, and IL-6) were decreased, as expected. These results are consistent with the reduced number of macrophages in the liver assessed by CD68 immunohistochemistry. Suppression of inflammation may be the beneficial result of attenuated hepatic steatosis. However, the mechanism of the blockade of intrahepatic inflammation by PREP knockdown needs further research.

Previous studies have shown that PREP and MMP8/MMP9 synergistically hydrolyze collagen to produce PGP, which regulates the chemotaxis of neutrophils via CXCR2 (12,13). Acetylation of PGP leads to N-Ac-PGP, which is a more potent chemoattractant for neutrophils than PGP itself (31). Neutrophils are the first responders in the inflammatory process of NAFLD progression to NASH (32). Macrophages are the major cell type involved in hepatocyte steatosis and progression of NASH inflammation (33). It is currently believed that the infiltration and activation of macrophages are neutrophil-dependent (34). Based on these studies, we hypothesized that PREP disruption inhibits the accumulation of hepatic macrophages by regulating the generation of PGP and neutrophil chemotaxis upon HFD stimulus. Our study demonstrates that MMP9 is significantly decreased in the HFD-PREP^{gt} mice. Previous studies indicated that PREP could regulate the activity of extracellular MMP9 (29,35). Notably, the production of PGP was obviously suppressed in the HFD-PREP^{gt} mice. This result might be explained by MMP8/9 downregulation and PREP disruption, which inhibited collagen hydrolysis. The endogenous ligands of

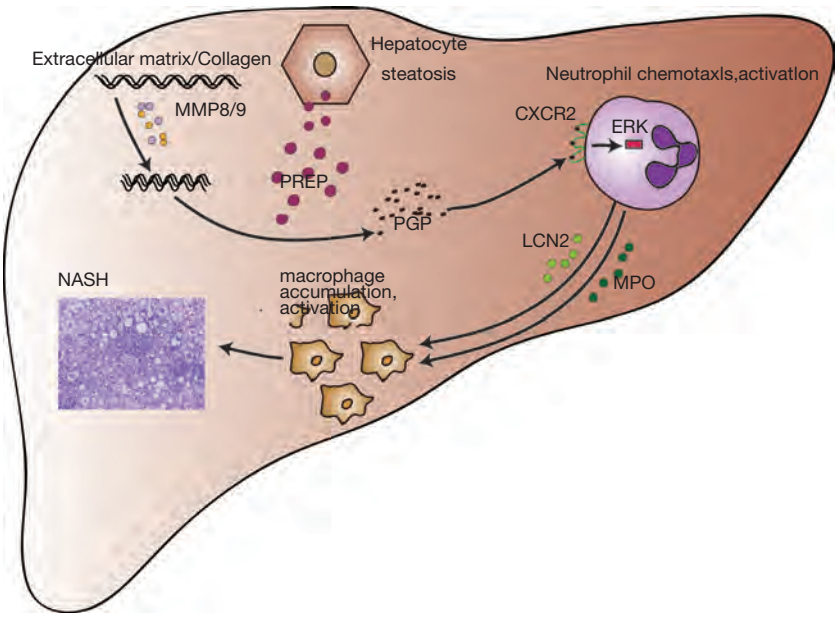

Figure 6 PREP can potentially affect the progression of hepatic inflammation, possibly by regulating chemotactic factors (such as PGP) and inflammatory cells accumulation.

CXCR2 in the liver, namely CXCL1 and CXCL2, were also improved in the HFD-PREP^{gt} mice. This is similar to the findings of a previous study, where the elevation of both CXCL1 and CXCL2 in *in vivo* models of colitis was reduced by PGP neutralization (16). Our present study also demonstrated a downregulated expression of CXCR2 in the livers of the HFD-PREP^{gt} mice. CXCR2 is a prominent chemokine receptor with pleiotropic effects on the regulation of neutrophil homeostasis. Induction of CXCR2 subsequently activates ERK and facilitates the crosstalk between neutrophils and macrophages to exacerbate their migration and activation (34). Activated neutrophils produce a large amount of MPO and LCN2, which induce cytotoxicity and inflammatory responses in macrophages (34,36). In support of this notion, our *in vivo* studies showed that the HFD-PREP^{gt} mice displayed reduced CXCR2 expression and suppression of ERK1/2. These results are consistent with the reduced number of neutrophils in the liver assessed by MPO and LCN2 immunohistochemistry. In summary, these results provide additional support to the hypothesis that PREP inhibitors can protect against the progression of hepatic inflammation, possibly by regulating chemotactic factors (such as PGP) and inflammatory cell accumulation (*Figure 6*).

Our study has certain limitations. First, we found that PREP disruption plays a beneficial role in lipid accumulation and hepatic inflammation, mainly through decreased PGP production, inhibition of neutrophil activation via CXCR2, and decreased macrophage infiltration and activation induced by MPO and LCN2 excreted by neutrophils (*Figure 6*). However, more detailed molecular mechanisms at the cellular level need to be explored and are warranted in the near future. Second, additional studies should be performed in human subjects.

In conclusion, our study shows that PREP disruption decreases the severity of hepatic steatosis and the inflammatory response in an HFD-induced NASH model. Future studies are warranted to define the mechanisms of action of PREP in the regulation of NASH progression. These results indicate that PREP inhibitors may offer a novel therapeutic approach for the treatment of NAFLD/NASH.

Acknowledgments

Funding: This work was supported by the National Natural Science Foundation of China, grants Nos. 81770575 and 81970511 (to YW Chen).

Footnote

Conflicts of Interest: The authors have no conflicts of interest to declare.

Ethical Statement: The authors are accountable for all aspects of the work in ensuring that questions related to the accuracy or integrity of any part of the work are appropriately investigated and resolved. All animal experiment protocols were approved by the Institutional Animal Care and Use Committee of Xinhua hospital affiliated to Shanghai Jiao Tong University School of Medicine (approval No. XHEC-F-2019-061).

References

1. Araújo AR, Rosso N, Bedogni G, et al. Global epidemiology of non-alcoholic fatty liver disease/non-alcoholic steatohepatitis: What we need in the future. Liver Int 2018;38 Suppl 1:47-51.
2. Yu Y, Cai J, She Z, et al. Insights into the Epidemiology, Pathogenesis, and Therapeutics of Nonalcoholic Fatty Liver Diseases. Adv Sci (Weinh) 2018;6:1801585.
3. Anstee QM, Reeves HL, Kotsiliti E, et al. From NASH to HCC: current concepts and future challenges. Nat Rev Gastroenterol Hepatol 2019;16:411-28.
4. Lonardo A, Nascimbeni F, Mantovani A, et al. Hypertension, diabetes, atherosclerosis and NASH: Cause or consequence? J Hepatol 2018;68:335-52.
5. Tilg H, Moschen AR, Roden M. NAFLD and diabetes mellitus. Nat Rev Gastroenterol Hepatol 2017;14:32-42.
6. Boyle M, Masson S, Anstee QM. The bidirectional impacts of alcohol consumption and the metabolic syndrome: Cofactors for progressive fatty liver disease. J Hepatol 2018;68:251-67.
7. Brunt EM, Wong VW, Nobili V, et al. Nonalcoholic fatty liver disease. Nat Rev Dis Primers 2015;1:15080.
8. Buzzetti E, Pinzani M, Tsochatzis EA. The multiple-hit pathogenesis of non-alcoholic fatty liver disease (NAFLD). Metabolism 2016;65:1038-48.
9. Suzuki A, Diehl AM. Nonalcoholic Steatohepatitis. Annu Rev Med 2017;68:85-98.
10. Rolo AP, Teodoro JS, Palmeira CM. Role of oxidative stress in the pathogenesis of nonalcoholic steatohepatitis. Free Radic Biol Med 2012;52:59-69.
11. Bastos IM, Motta FN, Grellier P, et al. Parasite prolyl oligopeptidases and the challenge of designing chemotherapeuticals for Chagas disease, leishmaniasis and African trypanosomiasis. Curr Med Chem 2013;20:3103-15.
12. Weathington NM, van Houwelingen AH, Noerager BD, et al. A novel peptide CXCR ligand derived from extracellular matrix degradation during airway inflammation. Nat Med 2006;12:317-23.
13. Gaggar A, Jackson PL, Noerager BD, et al. A novel proteolytic cascade generates an extracellular matrix-derived chemoattractant in chronic neutrophilic inflammation. J Immunol 2008;180:5662-9.
14. Penttinen A, Tenorio-Laranga J, Siikanen A, et al. Prolyl oligopeptidase: a rising star on the stage of neuroinflammation research. CNS Neurol Disord Drug Targets 2011;10:340-8.
15. Kim JD, Toda C, D'Agostino G, et al. Hypothalamic prolyl endopeptidase (PREP) regulates pancreatic insulin and glucagon secretion in mice. Proc Natl Acad Sci U S A 2014;111:11876-81.
16. Koelink PJ, Overbeek SA, Braber S, et al. Collagen degradation and neutrophilic infiltration: a vicious circle in inflammatory bowel disease. Gut 2014;63:578-87.
17. Tenorio-Laranga J, Montoliu C, Urios A, et al. The expression levels of prolyl oligopeptidase responds not only to neuroinflammation but also to systemic inflammation upon liver failure in rat models and cirrhotic patients. J Neuroinflammation 2015;12:183.
18. Kamori M, Hagihara M, Nagatsu T, et al. Activities of dipeptidyl peptidase II, dipeptidyl peptidase IV, prolyl endopeptidase, and collagenase-like peptidase in synovial membrane from patients with rheumatoid arthritis and osteoarthritis. Biochem Med Metab Biol 1991;45:154-60.
19. Zhou D, Li BH, Wang J, et al. Prolyl Oligopeptidase Inhibition Attenuates Steatosis in the L02 Human Liver Cell Line. PLoS One 2016;11:e0165224.
20. Shen B, Zhang J, Wu H, et al. Generation of gene-modified mice via Cas9/RNA-mediated gene targeting. Cell Res 2013;23:720-3.
21. Wang H, Yang H, Shivalila CS, et al. One-step generation

of mice carrying mutations in multiple genes by CRISPR/Cas-mediated genome engineering. Cell 2013;153:910-8.
22. Estes C, Razavi H, Loomba R, et al. Modeling the epidemic of nonalcoholic fatty liver disease demonstrates an exponential increase in burden of disease. Hepatology 2018;67:123-33.
23. Höfling C, Kulesskaya N, Jaako K, et al. Deficiency of prolyl oligopeptidase in mice disturbs synaptic plasticity and reduces anxiety-like behaviour, body weight, and brain volume. Eur Neuropsychopharmacol 2016;26:1048-61.
24. Sánchez-Garrido MA, Habegger KM, Clemmensen C, et al. Fibroblast activation protein (FAP) as a novel metabolic target. Mol Metab 2016;5:1015-24.
25. Bijnen M, Josefs T, Cuijpers I, et al. Adipose tissue macrophages induce hepatic neutrophil recruitment and macrophage accumulation in mice. Gut 2018;67:1317-27.
26. Schuster S, Cabrera D, Arrese M, et al. Triggering and resolution of inflammation in NASH. Nat Rev Gastroenterol Hepatol 2018;15:349-64.
27. Tenorio-Laranga J, Mannisto PT, Storvik M, et al. Four day inhibition of prolyl oligopeptidase causes significant changes in the peptidome of rat brain, liver and kidney. Biochimie 2012;94:1849-59.
28. Mahli A, Saugspier M, Koch A, et al. ERK activation and autophagy impairment are central mediators of irinotecan-induced steatohepatitis. Gut 2018;67:746-56.
29. Natunen TA, Gynther M, Rostalski H, et al. Extracellular prolyl oligopeptidase derived from activated microglia is a potential neuroprotection target. Basic Clin Pharmacol Toxicol 2019;124:40-9.
30. Klegeris A, Li J, Bammler TK, et al. Prolyl endopeptidase is revealed following SILAC analysis to be a novel mediator of human microglial and THP-1 cell neurotoxicity. Glia 2008;56:675-85.
31. Haddox JL, Pfister RR, Muccio DD, et al. Bioactivity of peptide analogs of the neutrophil chemoattractant, N-acetyl-proline-glycine-proline. Invest Ophthalmol Vis Sci 1999;40:2427-9.
32. Pernes G, Lancaster GI, Murphy AJ. Take me to the liver: adipose tissue macrophages coordinate hepatic neutrophil recruitment. Gut 2018;67:1204-6.
33. Kazankov K, Jorgensen SMD, Thomsen KL, et al. The role of macrophages in nonalcoholic fatty liver disease and nonalcoholic steatohepatitis. Nat Rev Gastroenterol Hepatol 2019;16:145-59.
34. Ye D, Yang K, Zang S, et al. Lipocalin-2 mediates non-alcoholic steatohepatitis by promoting neutrophil-macrophage crosstalk via the induction of CXCR2. J Hepatol 2016;65:988-97.
35. Jaako K, Waniek A, Parik K, et al. Prolyl endopeptidase is involved in the degradation of neural cell adhesion molecules in vitro. J Cell Sci 2016;129:3792-802.
36. Pulli B, Ali M, Iwamoto Y, et al. Myeloperoxidase-Hepatocyte-Stellate Cell Cross Talk Promotes Hepatocyte Injury and Fibrosis in Experimental Nonalcoholic Steatohepatitis. Antioxid Redox Signal 2015;23:1255-69.

Cite this article as: Jiang DX, Zhang JB, Li MT, Lin SZ, Wang YQ, Chen YW, Fan JG. Prolyl endopeptidase gene disruption attenuates high fat diet-induced nonalcoholic fatty liver disease in mice by improving hepatic steatosis and inflammation. Ann Transl Med 2020;8(5):218. doi: 10.21037/atm.2020.01.14

Supplementary

Methods

The PREP^{gt} mice used in this study carry a partial deletion in exon 3 of the PREP gene. Briefly, Cas9 mRNA and gRNA were obtained by *in vitro* transcription; the Cas9 mRNA and gRNA were microinjected into fertilized eggs of C57BL/6J mice to obtain F0 generation mice. The PCR products were sequenced to confirm that a total of two F0 generation mice with a frameshift mutation of the target protein were obtained. The F0 generation mice were mated with C57BL/6J mice to obtain a total of 4 positive F1 generation mice (heterozygote mice). Homozygous knockout mice were obtained by mating heterozygous mice.

Comparative genotypic analysis of knockout F1 mice

Sequence alignment before and after knockout: (Yellow highlights indicate gRNA target sites, red underlines indicate PAM sequences, and "-" indicate missing sequences).

Wild-type: accggctgtaagaatggggtcctactcctgccttaaccccaag gtctcctgatttcctgtgctccctttaaaccatgattgtggggctggagagatggctc agcggttaacagcactgaatgctctcctagtacccacgtggcagctcacgattgtctg agactccaaactctgacacctccatacaggcatacatgcaggcaaaacatcaatgtat ataaaataaacataaattcaatttaaaaaatgtgattgttggcattcttagtccctgcca cttcagttacacattttagtgaagttcttggttggagccgacatagcggtaggttttag ataccatgaggaaggaaggtcattgaaataatgcctaagtgttttctcctacatttgac ctggggcttgaagctggccctttggggatttataaatatgtatcactgatgggatatg actgagtagtgtggtacagtgtgtttgctaggaatgtagattcagaagccagatccac tccctcgctgtataatgttggatagcttttccgactacatcagtgtgcagctttcttata tgtaacagtggcttcctgagagaatctgcttgggctgcagagatggttcagttaacc ctgatgatctgagtcccatcctttgggacccatgtgatggaaggaaagaaacatctac aaattgtcccctgccatccacacaggtgctgtgggatgggcacgcacatgcgtgtgt gctagctttgaagtcactgtggtcctcctgcctcagcctcctgactgttggaattacag acaggagctgtcgtcacactcaattttccaaactatgcttctgttgattcgtgctaaag agtgatgcttcacgggggggagttttgtatttgacttgccttttgtccttttaattctctg cagGCTTTCGTGGAGGCACAAAACAAGATTACTGT GCCATTTCTTGAGCAATGTCCAATCAGAGGTTTA TACAAGGAGAGAATGACTGAGCTGTACGACTACC CCAAGTACAGCTGCCACTTCAAGAAAGGAAAGCG gtaggtgggcttgcatgtagtcctttgctttccactctccagcttgatgtcttctgtaaa agataaaagtgtatgttgtgtatgtgtgtgtgtgtgtgtgtgtgagagagagagag agagagagagagagagagagaatatgcacatgccagaggtttcttcctctatcatca tctctccccaccacccccctcattgagacagggtctttctgcatagctctctgactgtc ctagaactcacaggctggcctccaactcacagatgtccacctgcctctgcttcttgag tgctgggattaaaggctcaagccacaactttccttctgccctgtttttgagacaggct cgctctcagaacctggagtttaccagagcttggggtaagacatggcagccatggtg cctagcttttgtgtcagtgttggggattccagctcaggacttcatgcaatcgacatgtc acccgctgagccacctttcagctctcctgaatgcctgaaataccaaggacaagtgag gtgtggtgcacgccttttatctcagcacttgagatgcagagacaagtggctgtcttag ttctaggccagcctggtgcatagggagactccgtctcagacaaatgaagtacacattt gaactgagcagttttaaaaggaagtgattgaacatgagaatcatttttgtcccgcta agtgcttaccatattcatcaaatggcagttaggaagtttggcagtgatacagcctgtg aaactagattacggtaaatcttcgttacctgtggttacttggtgagcctgtgactcata agtaacagtgaagatttgtttccatgtaatatttattatctttggcttgtattacttgaaat attttattctttgagcttttt

Mutant (1,352 base pairs deleted): accggctgtaagaatgggg tcctactcctgccttaaccccaaggtctcctgatttcctgtgctccctttaaaccat gattgtggggct----------tggggtaagacatggcagccatggtgcctagcttttgtgtcagtgttggggattcca gctcaggacttcatgcaatcgacatgtcacccgctgagccacctttcagctctcctga atgcctgaaataccaaggacaagtgaggtgtggtgcacgccttttatctcagcacttg agatgcagagacaagtggctgtcttagttctaggccagcctggtgcatagggagac tccgtctcagacaaatgaagtacacatttgaactgagcagtttttaaaaggaagtgatt gaacatgagaatcatttttttgtcccgctaagtgcttaccatattcatcaaatggcagtta ggaagtttggcagtgatacagcctgtgaaactagattacggtaaatcttcgttacctgt ggttacttggtgagcctgtgactcataagtaacagtgaagatttgtttccatgtaatatt tattatctttggcttgtattacttgaaatattttattctttgagcttttt

Gene function analysis before and after knockout

In this strain of mice, before and after gene knockout, changes in the protein encoded by the target gene are as follows (red indicates start of the frameshift):

Wild-type: LSFQYPDVYRDETSVQEYHGHKICDP YSWLEDPDSEQTKAFVEAQNKITVPFLEQCPIRGLY KERMTELYDYPKYS……

Mutant: MLSFQYPDVYRDETSVQEYHGHKICDPY SWLEDPDSEQTKVLLFLQYRFAEPTRVICARLLRG GGQSVPGPQHTVG……

The frame of the target gene protein is frame-shifted and terminated early, which theoretically will produce a mutant protein of 76 amino acids; the early termination of protein translation of the target gene will most likely trigger the Nonsense-mediated mRNA decay (NMD) effect and cause Gene mRNA is degraded, resulting in loss of gene function (*Figure 1*).

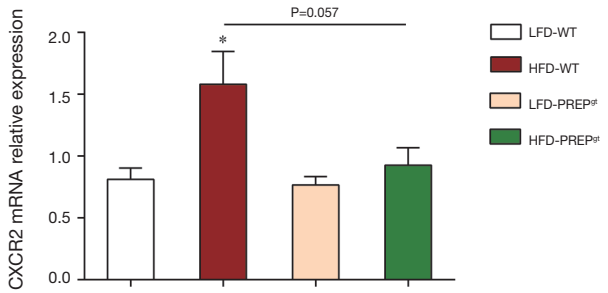

Figure S1 CXCR2 mRNA relative expression.

Table S1 List of primer sequences used for RT-PCR

Gene	Forward primer	Reverse primer
ACC	5′-TTGAAGGCACAGTGAAGGCTTACG-3′	5′-CCATCTTCCTCTGTCAGTTGCTTCTC-3′
SREBP1c	5′-GCGGCGGTTGGCACAGAG-3′	5′-CCTCCTCCTCAGACTGCGATCC-3′
SCD1	5′-CTACACCTGCCTCTTCGGGA-3′	5′-CACGTCATTCTGGAACGCCA-3′
FASN	5′-ACCACCCAGAAGTCCCAACA-3′	5′-CCCTGGAACTGAGGGCCATA-3′
CPT1a	5′-AGCCAGACTCCTCAGCAGCAG-3′	5′-CACCATAGCCGTCATCAGCAACC-3′
ACOX1	5′-GCCGCCGCCACCTTCAATC-3′	5′-ACTCTTCTTAACAGCCACCTCGTAAC-3′
CD36	5′-GCGACATGATTAATGGCACAGACG-3′	5′-CCGAACACAGCGTAGATAGACCTG-3′
FABP1	5′- TTTCAAAGGCATAAAGTCCGTG-3′	5′- CTTGCTGACTCTCTTGTAGACA-3′
PPAR-α	5′-ACGATGCTGTCCTCCTTGATGAAC-3′	5′-GATGTCACAGAACGGCTTCCTCAG-3′
PPAR-γ	5′-CGCCAAGGTGCTCCAGAAGATG-3′	5′-GGTGAAGGCTCATGTCTGTCTCTG-3′
CCL2	5′-CCACTCACCTGCTGCTACTCATTC-3′	5′-CTGCTGCTGGTGATCCTCTTGTAG-3′
CCR2	5′-GACAAGCACTTAGACCAGGCCATG-3′	5′-AGCTCACTCGATCTGCTGTCTCC-3′
CCL5	5′-CCGCACCTGCCTCACCATATG-3′	5′-CTTGGCGGTTCCTTCGAGTGAC-3′
TNF-α	5′-GCGACGTGGAACTGGCAGAAG-3′	5′-GAATGAGAAGAGGCTGAGACATAGGC-3′
IL-6	5′-ACTTCCATCCAGTTGCCTTCTTGG-3′	5′-TTAAGCCTCCGACTTGTGAAGTGG-3′
IL-1β	5′-TTCAGGCAGGCAGTATCACTCATTG-3′	5′-ACACCAGCAGGTTATCATCATCATCC-3′
CXCR2	5-GGGCTGCATCTAAAGTAAATGG-3′	5-CAGAACACTGCTGTAGAAGGTA-3′